Lu Chun
K. Y. Lam
Department of Mechanical & Production Engineering
National University of Singapore
10 Kent Ridge Crescent
Singapore 0511

Behavior of Uniform Anisotropic Beams of Rectangular Section under Transverse Impact of a Mass

A numerical method is presented to investigate the dynamic response of uniform orthotropic beams subjected to an impact of a mass. Higher order shear deformation and rotary inertia are included in the analysis of the beams. The impactor and laminated composite beam are treated as a system. The nonlinear differential governing equations of motion are then derived based on the Lagrange principle and modified nonlinear contact law, and solved numerically. The solution procedure is applicable to arbitrary boundary conditions. Numerical results are compared with those available in the literature to demonstrate the validity of the method, and very good agreement is achieved. The effects of boundary conditions on the contact force, contact duration, stress distributions, and beam deflection are discussed. © *1997 John Wiley & Sons, Inc.*

INTRODUCTION

The dynamic behavior of an isotropic beam when subjected to the transverse impact of a mass was first investigated by Timoshenko (1931). He studied steel beams elastically impacted by a steel ball. By combining the Hertzian contact law and Euler–Bernoulli beam theory, he simplified the impact phenomenon into a 1 degree of freedom model and obtained a nonlinear integral equation for the impact force; the resulting equation was then called Timoshenko's integral equation. The nonlinearity of the equation was caused by the nonlinear relationship between the impact force and the approach of the mass and beam. Timoshenko solved the equation by a stepwise numerical integration procedure and obtained the contact force; consequently the deflection of the beam and the displacement of the impactor were calculated. Later, a similar method was extended to study the dynamic response of other isotropic structural elements, such as plates and shells, under impact loading. Various simplified methods were also suggested to avoid the difficulty of nonlinearity in Timoshenko's integral equation.

Recently, advanced fiber-reinforced composite materials, such as graphite/epoxy, have been successfully utilized as structural materials for various industrial applications. The laminated composite structures are sensitive to impact loading that may cause invisible internal delaminations. The understanding of the dynamic impact response of structures is key to understanding the causes and prevention of damage. Therefore, the low-velocity impact problem of composite structures has become an important subject for research. A similar

Received October 27, 1994; Accepted October 30, 1996
Shock and Vibration, Vol. 4, No. 2, pp. 125–141 (1997)

CCC 1070-9622/97/020125-17

approach to Timoshenko's was adopted by most researchers to solve the problem of composite structures under impact of a mass. Most of these authors focused their attention on the dynamic impact response of laminated composite plates (Bogdanovich and Iarve, 1992; Chattopadhyay and Saxena, 1991; Christoforou and Swanson, 1991; Dobyn, 1981; Sun and Chattopadhyay, 1975), but only a few researchers tried to predict the dynamic response of laminated beams subjected to impact. Sun (1977) proposed a modified nonlinear contact law for orthotropic materials that accounted for the permanent indentation after unloading, and developed a finite element code to calculate the low velocity impact of composite beams. Schonberg, Keer, and colleagues (Keer and Balarini, 1983; Keer and Lee, 1985; Schonberg, 1989; Schonberg et al., 1987) studied the dynamic response of transverse isotropic beams subjected to impact loading by superimposing a static layer solution with the Euler–Bernoulli beam theory; however, the method could not be readily employed to analyze inhomogeneous materials. Xia (1988) presented an analysis of low-velocity impact on a two-layer beam with interlayer slip; his work was based on Timoshenko beam theory. For composite materials, the transverse shear deformations in some cases are significant due to the high ratio of the extension modulus to the transverse shear modulus. Both elementary and Timoshenko beam theories are therefore inadequate for accurate calculation of the response of composite beams under impact.

In the present work, a numerical method is presented to investigate the dynamic response of low-velocity impact on laminated beams with arbitrary boundary conditions. A higher order shear deformation theory is adopted for the analysis. Unlike most earlier studies on low-velocity impact, which tried to obtain an integral equation for the impact force, the impactor and laminated composite beam are treated as a system in the present analysis; hence, the impact force is an internal force in the system. In this case, the difficulty of solving a nonlinear integral equation is avoided. The potential and kinetic energies are expressed in terms of the generalized displacements of the laminated beam and the displacement of mass. By applying Lagrange's principle and using the modified contact law, the governing equations of motion can then be derived for the system; it should be noted that the governing equations are second-order differential equations. The equations of motion are then uncoupled by introducing the transformation of principal coordinates and solved by a numerical technique. Numerical results obtained in the present analysis are compared with those available in the literature to verify the applicability of the method. The dynamic response of cross-ply laminated beams subjected to the impact of a mass are presented. The effects of different boundary conditions, simply supported–simply supported (SS), clamped–clamped (CC), clamped–simply supported (CS), and clamped–free (CF), are also discussed.

PROBLEM FORMULATION

Consider a system that consists of a laminated beam and impactor. The x–y plane of the Cartesian coordinate system is located in the middle plane of the laminated beam, and the z axis is perpendicular to the x–y plane as shown in Fig. 1. The laminated beam is constructed of K orthotropic layers. The length, height, and width of the beam are L, h, and b, respectively, where both ratios of h/L and b/L are much smaller than unity. The impactor strikes the beam at x_s with the initial velocity V_0. The mass of the impactor is m_s. Following a procedure similar to Reddy's higher order shear deformation theory of plates (Reddy, 1984), in which the transverse shear stresses, $\sigma_{xz} = \sigma_5$ and $\sigma_{zy} = \sigma_4$, vanish on the plate's top and bottom surfaces, the assumed displacement field for the laminated beam is taken to be of the form

$$u(x, z, t) = u_0(x, t) + z\psi_x(x, t) - \frac{4z^3}{3h^2}\left(\psi_x + \frac{\partial w}{\partial x}\right),$$
$$w(x, z, t) = w_0(x, t), \tag{1}$$

where u_0 and w_0 are the displacements of a point on the midplane and ψ_x is the rotation of the normal to the midplane about the y axis.

The strain–displacement relationships associated with the assumed displacements field in Eq. (1) are given by

$$\varepsilon_1 = \varepsilon_1^0 + z\kappa_1^0 + z^3\kappa_1^2,$$
$$\varepsilon_5 = \varepsilon_5^0 + z^3\varepsilon_5^2, \tag{2}$$

where

$$\varepsilon_1^0 = \frac{\partial u_0}{\partial x}; \quad \kappa_1^0 = \frac{\partial \psi_x}{\partial x}; \quad \kappa_1^2 = -\frac{4}{3h^2}\left(\frac{\partial \psi_x}{\partial x} + \frac{\partial^2 w}{\partial x^2}\right);$$
$$\varepsilon_5^0 = \psi_x + \frac{\partial w}{\partial x}; \quad \kappa_5^2 = -\frac{4}{h^2}\left(\psi_x + \frac{\partial w}{\partial x}\right). \tag{3}$$

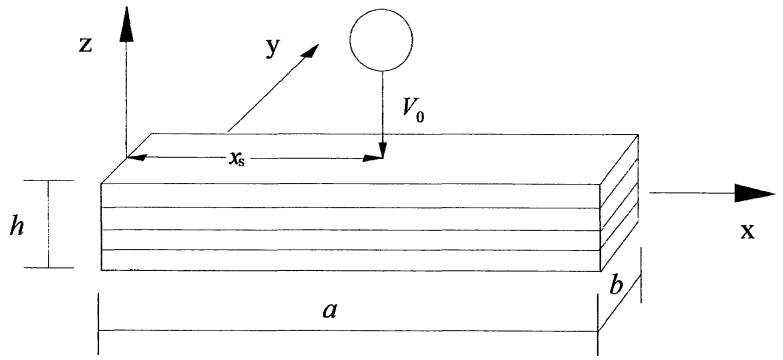

FIGURE 1 The geometrical configuration of the beam–impactor system.

By utilizing Hooke's law, the stresses in the kth layer of the laminated beam can be obtained in the following matrix form as

$$\begin{bmatrix} \sigma_1 \\ \sigma_5 \end{bmatrix}_k = \begin{bmatrix} Q_{11}^k & 0 \\ 0 & Q_{55}^k \end{bmatrix} \begin{bmatrix} \varepsilon_1 \\ \varepsilon_5 \end{bmatrix}_k, \tag{4}$$

where Q_{11}^k and Q_{55}^k are the transformed material constants given by

$$\begin{aligned} Q_{11}^k &= \overline{Q}_{11}^k \cos^4 \theta_k + \overline{Q}_{22}^k \sin^4 \theta_k \\ &\quad + 2(\overline{Q}_{12}^k + 2\overline{Q}_{66}^k) \sin^2 \theta_k \cos^2 \theta_k, \\ Q_{55}^k &= \overline{G}_{13}^k \cos^2 \theta_k + \overline{G}_{23}^k \sin^2 \theta_k, \end{aligned} \tag{5}$$

and θ_k is the angle between the fiber direction and x axis of the kth layer. $\overline{Q}_{ij}$ and $\overline{G}_{ij}$ are the material constants in the material coordinate system of the layer.

When the laminated beam is impacted by a mass an impact force results, and the value of the constant force is evaluated by a contact law that relates the impact force with indentation. Based on static indentation tests, Yang and Sun (1982) proposed a contact power law for composite materials in which permanent deformation at the contact point after a loading–unloading cycle was considered. In the present study, this modified contact law is used to predict the contact force between the laminated beam and impactor.

The contact force f_c is given as follows:

$$f_c = K_c(\alpha - \alpha_c)^{q_c}; \tag{6}$$

loading,

$$K_c = k_c, \quad \alpha_c = 0, \quad q_c = 1.5; \tag{7}$$

unloading,

$$K_c = \frac{F_m}{(\alpha_m - \alpha_0)^{2.5}}, \quad \alpha_c = \alpha_0, \quad q_c = 2.5; \tag{8}$$

reloading,

$$K_c = \frac{F_m}{(\alpha_m - \alpha_0)^{1.5}}, \quad \alpha_c = \alpha_0, \quad q_c = 1.5. \tag{9}$$

In the above equations, k_c is a modified contact constant, α_m is the maximum indentation during loading, F_m is the maximum contact force at the beginning of unloading, and α_0 is permanent indentation. The relative approach α can be expressed in terms of displacement of the laminated beam and the mass,

$$\alpha = w(x_s) - W_s, \tag{10}$$

where W_s is the displacement of the mass measured from the position of initial contact, and $w(x_s)$ is the deflection of the beam at the impact point x_s.

The response of the laminated beam under the impact force can be separated into functions of time and position. The displacement of the middle plane along the x direction, midplane slope, and transverse displacement of the beam are expressed by the matrix form,

$$\begin{bmatrix} u_0 \\ \psi_x \\ w \end{bmatrix} = \begin{bmatrix} [\phi_{ui}(x)] & 0 & 0 \\ 0 & [\phi_{xi}(x)] & 0 \\ 0 & 0 & [\phi_{zi}(x)] \end{bmatrix} \begin{bmatrix} [A_i(t)] \\ [B_i(t)] \\ [C_i(t)] \end{bmatrix},$$
$$i = 1, 2, \ldots, n, \tag{11}$$

where $A_i(t)$, $B_i(t)$, and $C_i(t)$ are defined as the generalized displacements of the laminated beam; $[\phi_{ui}(x)]$, $[\phi_{xi}(x)]$, and $[\phi_{zi}(x)]$ are three complete function series that satisfy the associated displacement boundary conditions; and n is the number of terms for series truncation. Equation (11) transforms a continuous system into a discrete system with $3n$ degrees of freedom.

To avoid solving a nonlinear integral equation in the determination of the impact force, the laminated beam and the mass are considered to be a system. The impact force becomes an internal force in the system. When the duration of the impact is long when compared to the period of the fundamental mode of the impactor, the vibration of the impactor is negligible (Rayleigh, 1906). Then the work done by the impact force is

$$P_c = \int_0^a f_c \, d\alpha = \frac{K_c}{(q_c + 1)} (\alpha - \alpha_c)^{q_c+1}. \tag{12}$$

By combining Eqs. (10) and (12), the kinetic and potential energies of the system are given by

$$T = \frac{1}{2} \sum_{k=1}^{K} \int_{V_k} \rho_k [\dot{U}]^T [\dot{U}] \, dV + \frac{1}{2} m_s \dot{W}_s^2,$$
$$P = \frac{1}{2} \sum_{k=1}^{K} \int_{V_k} [\sigma]_k^T [\varepsilon]_k \, dV + \frac{K_c}{q_c + 1} (w(x_s) - W_s - \alpha_c)^{q_c+1}, \tag{13}$$

where $[U] = [u \quad w]^T$ and the superscript dot denotes the derivative with respect to time and ρ_k is the density of the kth layer.

The governing equations of motion for the system can be derived by applying Lagrange's equations:

$$\frac{d}{dt}\left[\frac{\partial L}{\partial \dot{p}_j}\right] - \frac{\partial L}{\partial p_j} = 0, \quad j = 1, 2, \ldots, 3n + 1, \tag{14}$$

where $L = T - P$ is defined as the Lagrangian and $[p_j] = [[A_i] \quad [B_i] \quad [C_i] \quad W_s]$ are $3n + 1$ generalized coordinates of the system. By placing Eqs. (1), (2), (4), and (13) into Eq. (14), collecting the coefficients of the generalized displacements of the system and nonlinear terms, the governing equations in terms of generalized displacements of the system are obtained as

$$\begin{bmatrix} [M] & [0]_d \\ [0]_d & m_s \end{bmatrix} \begin{bmatrix} [\ddot{A}_i(t)] \\ [\ddot{B}_i(t)] \\ [\ddot{C}_i(t)] \\ \ddot{W}_s(t) \end{bmatrix} + \begin{bmatrix} [K] & [k'] \\ [0]_d & -K_c \end{bmatrix} \begin{bmatrix} [A_i(t)] \\ [B_i(t)] \\ [C_i(t)] \\ \left(\sum_{i=1}^{n} C_i \phi_{zi}(x_s) - W_s - \alpha_c\right)^{q_c} \end{bmatrix} = [0], \tag{15}$$

where

$$[k'] = [[0]_e \quad [0]_e \quad K_c[\phi_{zi}(x_s)]]^T, \tag{16}$$

and $[M]$ and $[K]$ are the mass and stiffness matrices given in the Appendix and $[0]_d$ and $[0]_e$ are $3n \times 1$, $n \times 1$ zero matrices, respectively.

The laminated beam is assumed at rest when the mass strikes it. The initial conditions for the system are therefore given as

$$[U] = [\dot{U}] = [0], \quad W_s = 0, \quad \dot{W}_s = V_0. \tag{17}$$

From Eqs. (15) and (17) the response of the laminated beam and the displacement of the impactor can be determined. Due to the nonlinear terms in Eq. (15), closed form solutions cannot be expected. Hence, numerical techniques are employed.

SOLUTION PROCEDURE

The second derivative terms are coupled in the governing equation, Eq. (15). Before solving the governing equations of motion by numerical techniques, these second-order terms must be uncoupled. The mass matrix in Eq. (15) needs to be transformed into a diagonal matrix. By rearranging the governing equations of motion, the following form of the equations is obtained:

$$[M]\begin{bmatrix}[\ddot{A}_i(t)]\\ [\ddot{B}_i(t)]\\ [\ddot{C}_i(t)]\end{bmatrix} + [K]\begin{bmatrix}[A_i(t)]\\ [B_i(t)]\\ [C_i(t)]\end{bmatrix} \tag{18a}$$

$$= -[k']\left(\sum_{i=1}^{n} C_i\phi_{zi}(x_s) - W_s - \alpha_c\right)^{q_c},$$

$$m_s\ddot{W}_s = K_c\left(\sum_{i=1}^{n} C_i\phi_{zi}(x_s) - W_s - \alpha_c\right)^{q_c}. \tag{18b}$$

By setting the right side of Eq. (18a) to equal zero, Eq. (18a) can be used to determine the free vibration of the laminated beam with the corresponding boundary conditions. The frequencies and normalized mode shape matrix of the laminated beam are denoted by ω_i and $[V]$, respectively. If repeated frequencies occur, the associated modes are orthogonalized. Therefore, the orthogonality conditions are given by

$$[V]^T[M][V] = [I], \tag{19a}$$

$$[V]^T[K][V] = [\omega_i^2], \tag{19b}$$

where $[I]$ is the identity matrix, $[\omega_i^2]$ is the diagonal matrix, and its diagonal elements consist of $3n$ frequencies of the laminated beam.

The governing equations can then be uncoupled by introducing the transformation of principal coordinates:

$$\begin{bmatrix}[A_i(t)]\\ [B_i(t)]\\ [C_i(t)]\end{bmatrix} = \begin{bmatrix}[V_1]\\ [V_2]\\ [V_3]\end{bmatrix}[q_j(t)], \tag{20}$$

where $[V] = [[V_1]\ \ [V_2]\ \ [V_3]]^T$ and $q_j(t)(j = 1, 2, 3, \ldots, 3n)$ is called the principal coordinates of the laminated beam.

In the Eq. (18) the generalized transverse displacements $C_i(t)$ are included in the nonlinear terms. To express the governing equations in terms of the principal coordinates of the beam and the displacement of the impactor, $C_i(t)$ are written as

$$C_i(t) = \sum_{j=1}^{3n} V_3^{ij} q_j(t). \tag{21}$$

By substituting Eqs. (20) and (21) into (18), and multiplying $[V]^T$ on both sides, the uncoupled governing equations are obtained:

$$[\ddot{q}_i(t)] = -[V]^T[k']\left(\sum_{i=1}^{n}\sum_{j=1}^{3n} V_3^{ij}\phi_{zi}(x_s)q_j(t) - W_s - \alpha_c\right)^{q_c} - [\omega_i^2 q_i(t)], \tag{22a}$$

$$\ddot{W}_s = \frac{K_c}{m_s}\left(\sum_{i=1}^{n}\sum_{j=1}^{3n} V_3^{ij}\phi_{zi}(x_s)q_j(t) - W_s - \alpha_c\right)^{q_c}, \tag{22b}$$

where $[\ddot{q}_i] = [\ddot{q}_1\ \ \ddot{q}_2\ \cdots\ \ddot{q}_{2n}]^T$ and $[\omega_i^2 q_i] = [\omega_1^2 q_1\ \ \omega_2^2 q_2\ \cdots\ \omega_{2n}^2 q_{2n}]^T$.

The initial conditions for the principal coordinates of the beam can then be derived from Eqs. (17) and (20) as follows:

$$[q] = [\dot{q}] = [0]. \tag{23}$$

The initial value problem of Eqs. (22) and (23) is solved numerically using the Runge–Kutta–Nystron method (NAG, 1991). By choosing the appropriate function series $[\phi_{ui}(x)]$, $[\phi_{xi}(x)]$, and $[\phi_{zi}(x)]$ to satisfy the various boundary conditions, the numerical solutions of the dynamic response of the laminated beam with arbitrary boundary conditions are obtained. In the present study, simple-polynomial series are used to construct the functions $[\phi_{ui}(x)]$, $[\phi_{xi}(x)]$, and $[\phi_{zi}(x)]$, and the response of the cross-ply beam with SS, CC, CS, CF boundary conditions are calculated. Once the principal coordinates $q_i(t)$ are known, the deflection of the beam is calculated from Eqs. (11) and (20); the strains and stresses at any point of the beam are then obtained from Eqs. (2) and (4) according to the known displacements of the beam. From the governing equations, the displacement, velocity, and acceleration of the impactor are solved directly. The contact force and energy transformation between the laminated beam and impactor are obtained from Eqs. (6) and (13).

NUMERICAL RESULTS AND DISCUSSION

To verify the validity of the present method, numerical examples are given and compared, where possible, with those available in the literature. The impact of a mass on a laminated composite beam is then studied in detail.

Impact Between Isotropic Beam and Sphere

Consider a steel beam impacted elastically by a steel ball at the center point of the beam. Timo-

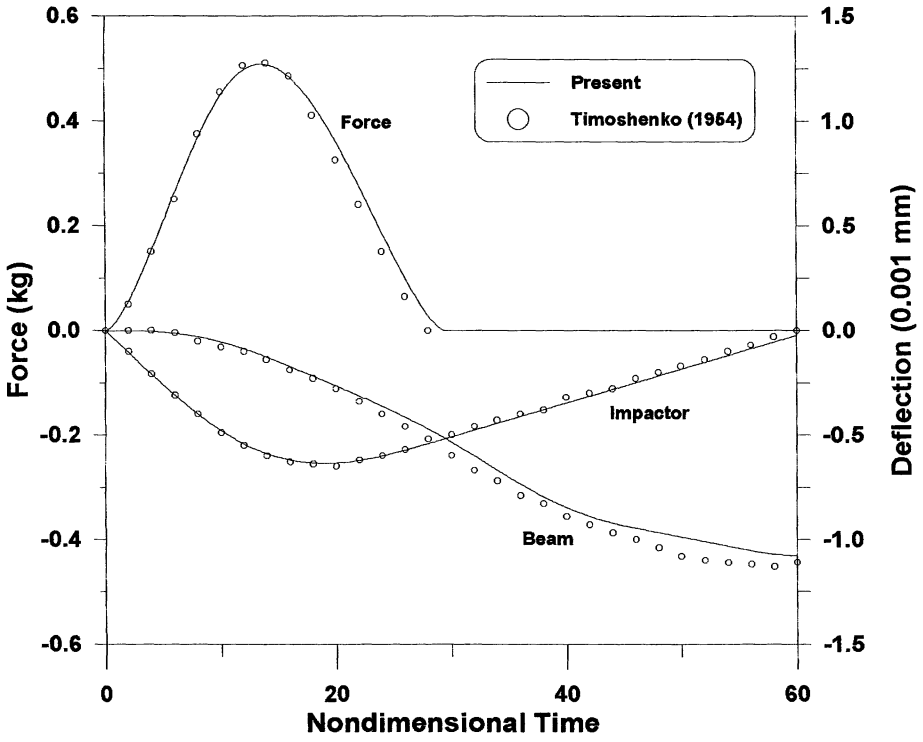

FIGURE 2 The comparison of the contact force and displacements for Timoshenko's case 1.

shenko initiated the method into the area by solving the same problem in 1931. In his investigation, two cases were considered. In the first case he studied a $1 \times 1 \times 15.35$ cm simply supported steel beam subjected to the transverse impact of a steel sphere with radius 1 cm at a velocity of 1 cm/s. The contact force and displacements of the sphere and the beam at the contact point were given in his publications (Timoshenko, 1931; Timoshenko and Young, 1954). In the second case the length of the beam and the radius of the sphere were taken to be twice as large as in the first case. A multiple-impact phenomena was found in the second case. The material constants of the steel are

$$E = 215.6 \text{ GPa}, \quad G = 80 \text{ GPa},$$
$$\rho = 7.96 \times 10^3 \text{ kg/m}^3, \quad \nu = 0.3,$$

where E and G are the Young's and shear moduli of steel and ρ and ν are the steel's density and Poisson ratio.

Numerical results calculated from the present formulation are compared with Timoshenko's solutions for the two cases and are plotted in Figs. 2 and 3. In Fig. 2 the histories of the contact force and displacements of the sphere and beam at the impact point are given for the first case. The circles in the figures represent Timoshenko's solutions. The kilogram is adopted as the unit of the contact force, and the nondimensional time τ is defined as $\tau = t/T'$, where T' is 1/180 of the fundamental natural period of the beam vibration (Timoshenko and Young, 1954). The figures show that very good agreement was achieved. For the second case, the histories of contact force, displacement of the impactor, and the deflection of the beam at the middle are plotted in Fig. 3. Timoshenko's only predicted that double impact occurred in this case; he then perhaps stopped further calculation when he found that the impactor reversed its velocity direction and separated from the beam after the second impact. Figs. 2 and 3 show that during the second impact the impactor reverses its direction of motion and separates from the beam after the maximum value of the contact force is achieved. When the maximum deflection of the beam is reached, the beam releases its stored energy and moves toward its initial position. The third impact happens when the impactor is caught by the beam before the beam and the impactor return to their position at $\tau = 0$. For the first two impacts, the present results are in good agreement with Timoshenko's solutions.

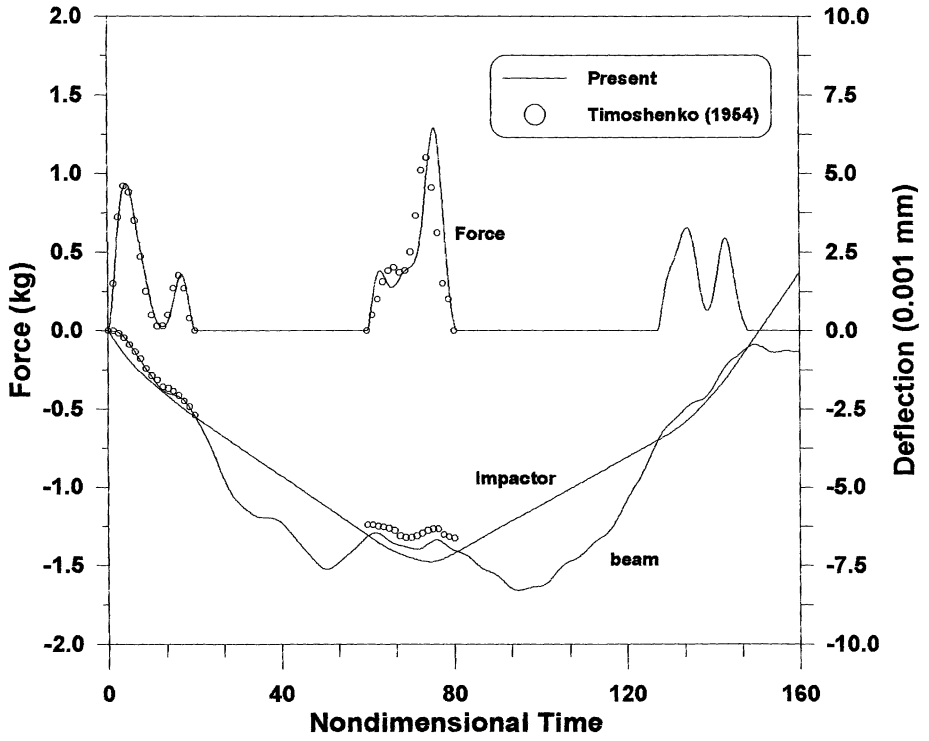

FIGURE 3 The comparison of the contact force and displacements for Timoshenko's case 2.

For the two cases, the ratios of the energy lost from the impactor and absorbed by the beam to the total energy of the system are plotted in Figs. 4 and 5 as a function of time. The vertical distances between the two energy ratio curves denote the fraction of the energy stored by the local deformation. In the second case the energy forming the local deformation reaches a maximum value during the second impact, and the potential energy stored in the beam is transmitted back to the steel ball during the third impact. After the impact, the energies lost from the impactor are 91 and 12% for case 1 and case 2, respectively. The phenomena can also be seen from the histories of the impactor velocity shown in Figs. 4 and 5. The rebound velocities are 0.3 cm/s in case 1 and 0.94 cm/s in case 2.

Goldsmith (1960) calculated the response of a steel beam when struck by a steel ball by using a dynamic plastic force–indentation law, in which a permanent crater at the impact point of the beam was considered. The steel beam has the dimensions 1.27 × 1.27 × 76.2 cm. The steel ball with radius 0.635 cm strikes the midspan of the simply supported beam at the initial velocity of 45.72 m/s. In Goldsmith's example, the force–indentation law was taken to be of the form

$$f_c = 3.616 \times 10^8 \alpha^{1.128}, \qquad 0 \le \alpha \le \alpha_m;$$
$$f_c = F_m \left(\frac{\alpha - 3.12 \times 10^{-4}}{\alpha_m - 3.12 \times 10^{-4}} \right)^{1.5}, \qquad (24)$$
$$\alpha_m \le \alpha \le 3.12 \times 10^{-4}.$$

The results obtained by combining the present formulation with the Hertzian law and the force–indentation contact law are given in Figs. 6 and 7. The contact forces, displacements of the impactor, and the deflections of the beam at the impact point obtained from Goldsmith are also plotted with open circles for comparison. The overall behavior exhibits good agreement in the two examples. The histories of the velocities of the impactor and the energy ratios are presented in Figs. 8 and 9. In the second case 82% of the initial kinetic energy carried by the steel ball is used to form the permanent crater in the impact point as indicated in Fig. 9.

Impact Between Laminated Composite Beam and Mass

With accuracy of the present method established, a laminated beam with boundary conditions of SS,

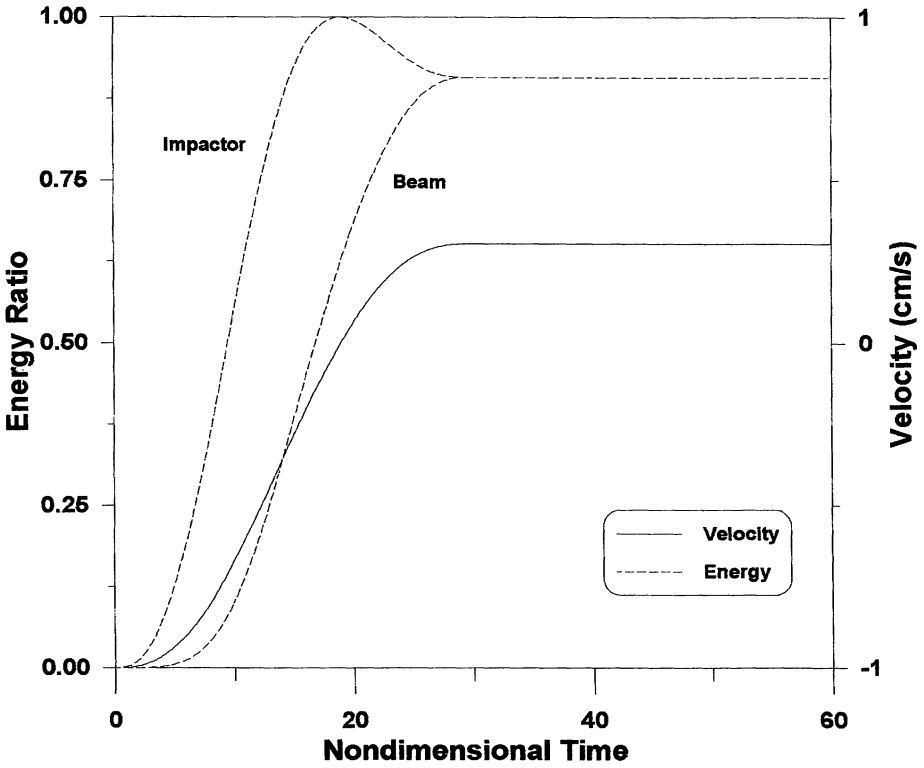

FIGURE 4 The energy ratios and the velocity for Timoshenko's case 1.

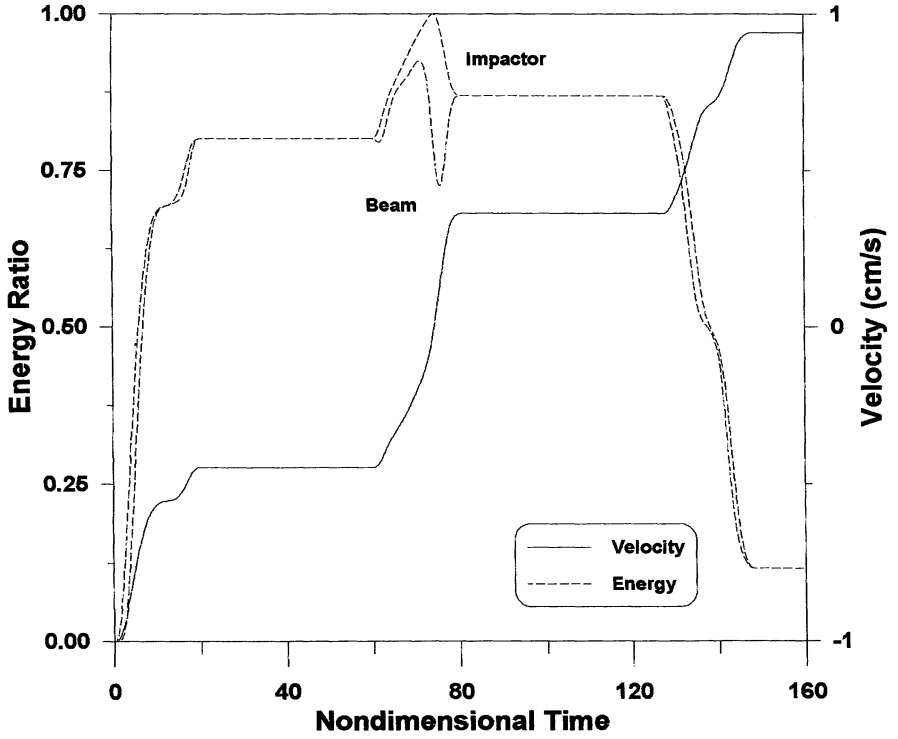

FIGURE 5 The energy ratios and the velocity for Timoshenko's case 2.

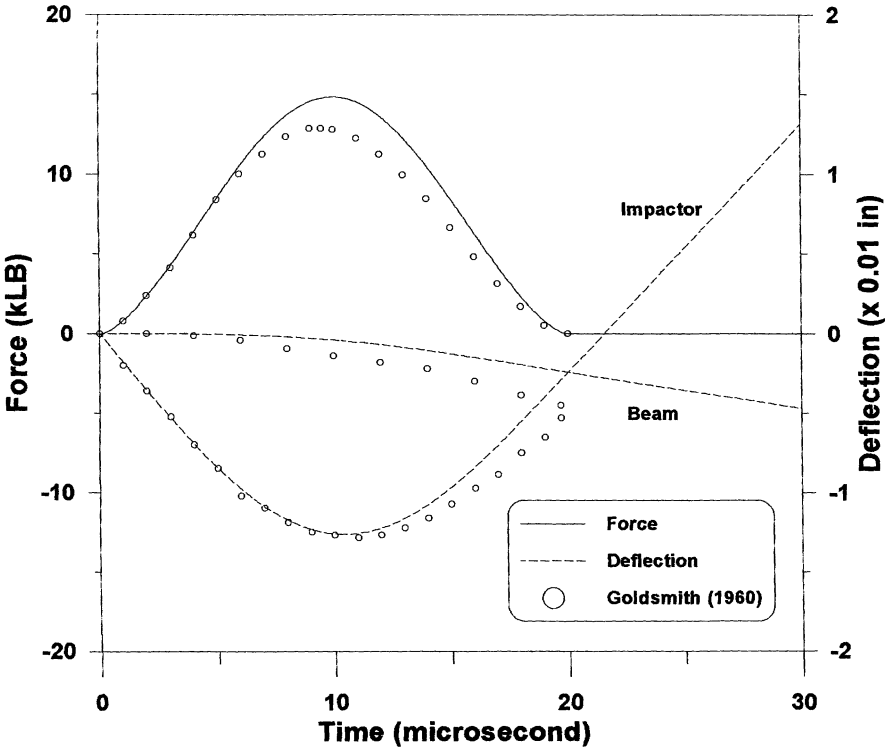

FIGURE 6 The contact force and displacements by Hertzian law.

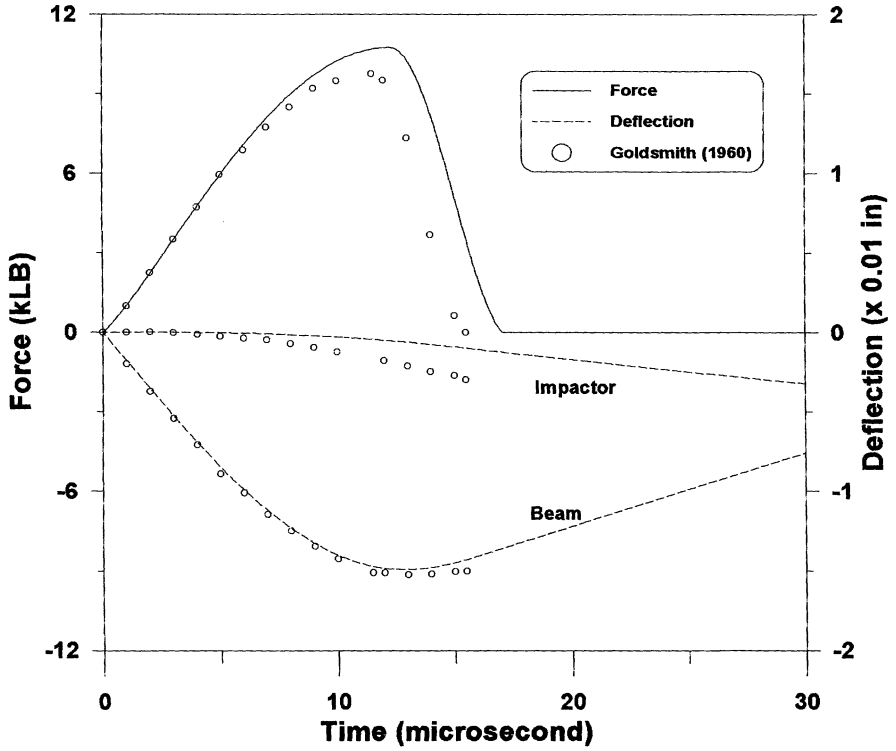

FIGURE 7 The contact force and displacements by force–indentation contact law.

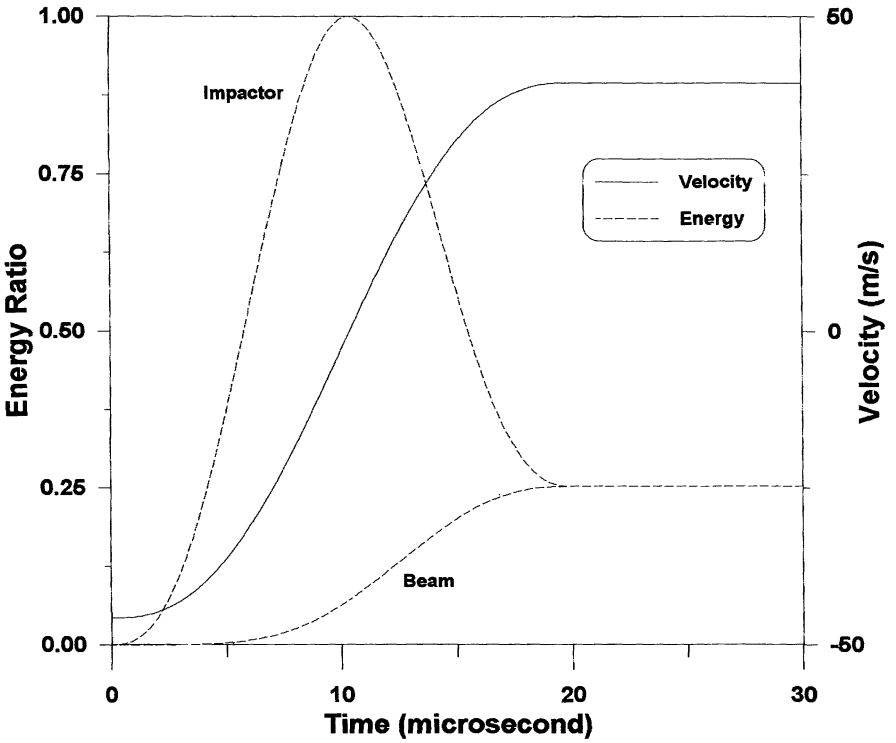

FIGURE 8 The energy ratios and the velocity by Hertzian law.

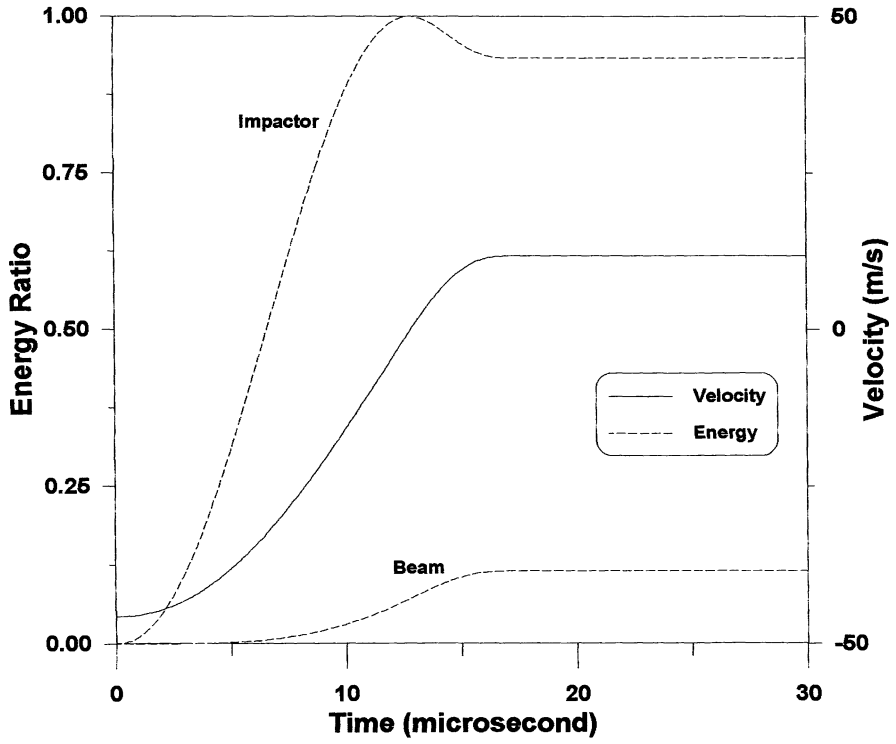

FIGURE 9 The energy ratios and the velocity by force–indentation contact law.

CC, CS, and CF is analyzed to demonstrate the influence of various boundary conditions on the transient response of the beam subjected to impact load. The contact force and duration, deflection of the beam at the contact point, energy transmission, and stresses histories are discussed.

The cross-ply laminated beam with a [0/90/90/0] lay-up is made of graphite/epoxy. Each lamina has the same thickness. The details of the geometrical configuration and the material constants are given as follows:

$$E_1 = 120\ \text{GPa}, \quad E_2 = 7.9\ \text{GPa},$$
$$G_{12} = G_{23} = G_{13} = 5.5\ \text{GPa},$$
$$\nu_{12} = 0.3, \quad \rho = 1.61 \times 10^3\ \text{kg/m}^3,$$
$$L = 20\ \text{cm}, \quad b = 2\ \text{cm}, \quad h = 1\ \text{cm}.$$

A steel impactor with a contacting spherical cap of radius 0.635 cm impacts the center point, ($L/2$, $b/2$), of the top surface of the laminated beam with an initial velocity of 10 m/s. The boundary conditions considered are simply supported at both ends, clamped at both ends, CS, and CF. The coefficients in the contact law, Eq. (6), are assumed as, loading,

$$k_c = 1.46 \times 10^9\ \text{N/m}^{1.5}, \quad q_c = 1.5;$$

unloading,

$$q_c = 2.5, \quad \alpha_c = 0.094(\alpha_m - 1.65 \times 10^{-5}), \quad \alpha_m \geq 1.65 \times 10^{-5}\ \text{m};$$
$$q_c = 2.5, \quad \alpha_c = 0, \quad \alpha_m < 1.65 \times 10^{-5}\ \text{m}.$$

The free vibration of the beam is first analyzed. The natural periods for the boundary conditions CC, CS, SS, and CF are 524.7, 729.7, 1099.7, and 3049.3 μs, respectively. The dynamic response of the beam under the impact of a mass is studied based on the vibration characteristics of the beam. The results for the contact forces are plotted in Figs. 10 and 11 for the four types of boundary conditions. The figures demonstrated that multiple impacts occur in all four boundary conditions. In the first impact, the magnitudes and durations of the contact forces are very close for four cases. The effects of the boundary conditions are reflected by the intervals, peak values, and numbers of the consequent impacts. For the beam fixed at both ends, which is stiffer when compared with the other three cases, only the double impacts occur and the second peak value of the contact force is larger than those in the other three cases. In the present problem the multiple impacts are mainly caused by the high frequency vibrations of the beam that are induced by the first impact. Similar multiple-impact phenomena were also found by Cairns and Lagace (1989) when they investigated the impact problem of composite plates with various boundary conditions.

The nondimensional displacements of the impactor and the deflections of the beam at the middle span are presented in Figs. 12 and 13 as a function of time. As can be seen, the high frequency vibrations of the beam are produced after the first contact. The reason is that the duration of the first impact is shorter than the natural periods of the beam with four boundary conditions. When the dotted line is above the solid line in Figs. 12 and 13, the impactor is separated from the beam. Also, in all four cases the impactors have not reached the maximum displacements in the negative z direction after the first contact. This implies that the velocity direction of the impactor is not reversed and only part of the initial kinetic energy is transmitted to the beam in the first impact process.

The in-plane stress σ_1 and transverse shear stress σ_5 at the midthickness of the bottom layer below the impact point are shown in Figs. 14 and 15 with respect to the various boundary conditions. The in-plane stresses σ_1 is much greater in magnitude than the transverse shear stress σ_5 for the four cases. At the considered point, the maximum σ_1 for the simply supported boundary condition is larger than those in other cases. This is because the resistance of the rotation of the cross sections to y axis in the simply supported beam is small when compared with the beam fixed by a clamped end. Due to the symmetry of the CC and SS beam according to the considered point, the transverse shear stress σ_5 at the considered point are zero in these two cases; the impact loading is supported by the in-plane deformation. For the beam with CS and CF boundary conditions, both σ_1 and σ_5 at the considered point are produced by the impact and the impact loading is supported by the in-plane and shear deformations. It is also worth noting that σ_1 and σ_5 undergo high frequency oscillations during the impact process and the higher modes become pronounced. The effect of higher modes may cause delamination damage in the composite beam.

CONCLUSION

A numerical method is presented by considering the beam and the impactor as a system. The high-

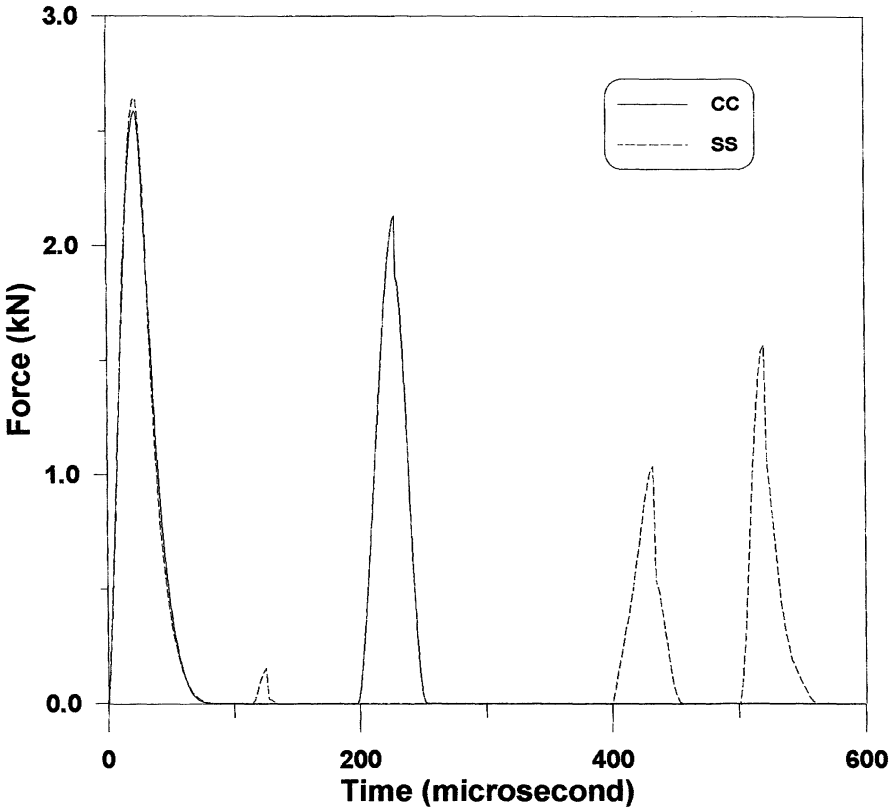

FIGURE 10 The contact forces in CC and SS.

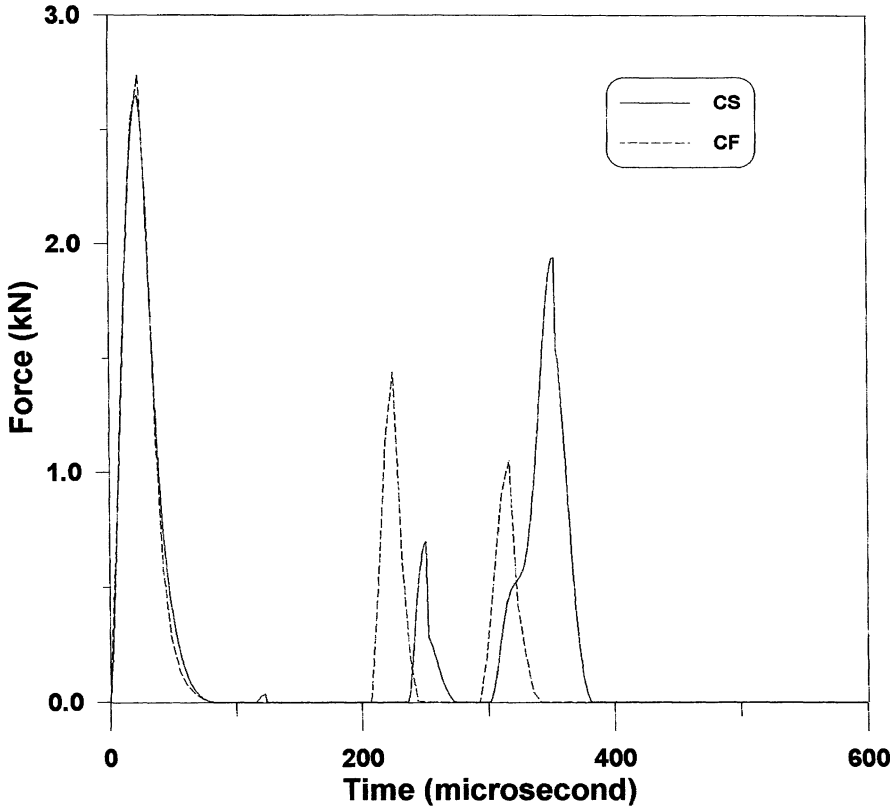

FIGURE 11 The contact forces in CS and CF.

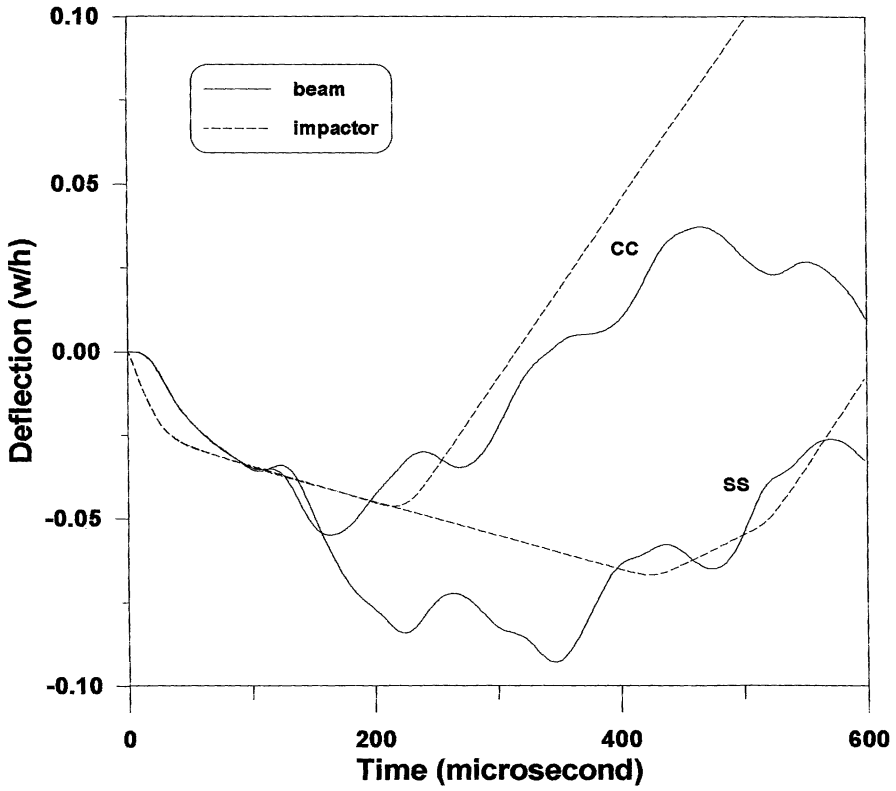

FIGURE 12 The displacements of the impactor and the laminated beam at the contact point in CC and SS.

order shear deformation and rotary inertia are included in the analysis of the beam. A set of governing equations of motion are obtained based on the Lagrange Principle and the plastic force–indentation law. The governing equations are discretized from a continuous system to a system with multiple degrees of freedom by a separating variables method. By introducing the principal coordinates transformation, the equations of motion for the system are uncoupled according to the second derivative terms and are then solved numerically by employing the Runge–Kutta–Nystron method.

The accuracy of the proposed method is verified by comparing the numerical results with the published solutions by Timoshenko (1954) and Goldsmith (1960). In one case that Timoshenko investigated by solving a nonlinear integral equation by using stepwise numerical integration, the present calculations predict that the third hit occurs during the impact process but Timoshenko gave only the first two impacts. The capability of the present formulation to combine with the various force indentation laws is examined by using Goldsmith's example, in which the permanent local deformation is taken into account.

The impact response of a laminated composite beam with a cross-ply layup is investigated with respect to the various boundary conditions. In this problem, the multiple impacts phenomena is observed in all cases.

From the numerical results, the following main points can be drawn:

1. The present method, combined with the proper contact law, can be used to study the dynamic response of the isotropic and composite structures under low-velocity impact.
2. The multiple impacts may occur in both isotropic and composite structures. Some simplified methods that assume one contact are no longer suitable for this kind of problem.
3. The influence of the boundary condition on the contact force, deflection, and stresses of the beam are considerable.

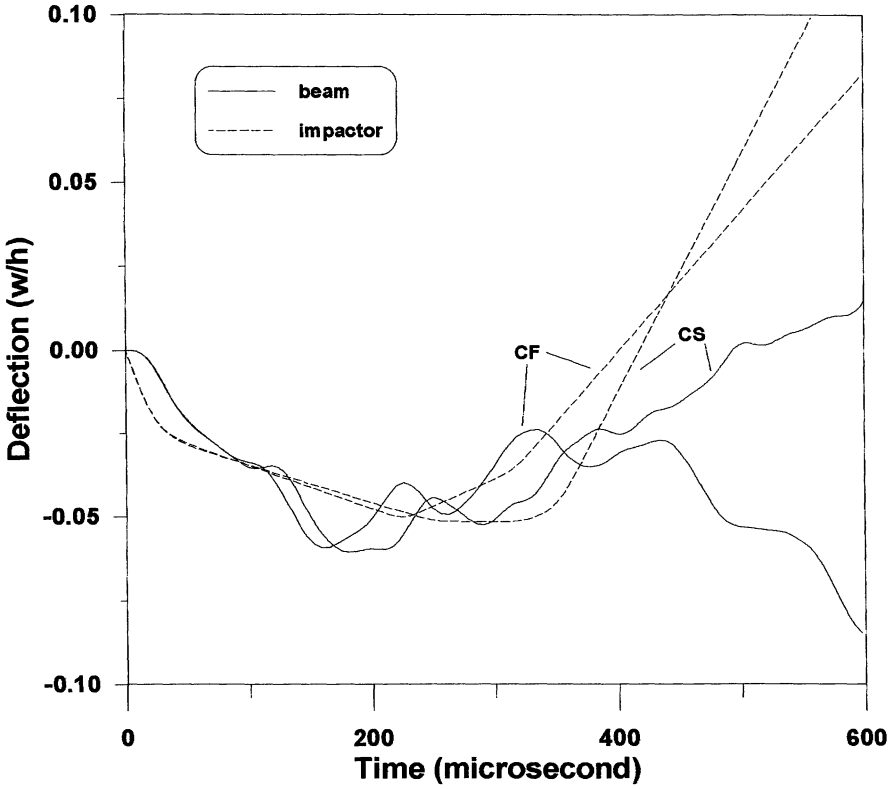

FIGURE 13 The displacements of the impactor and the laminated beam at the contact point in CS and CF.

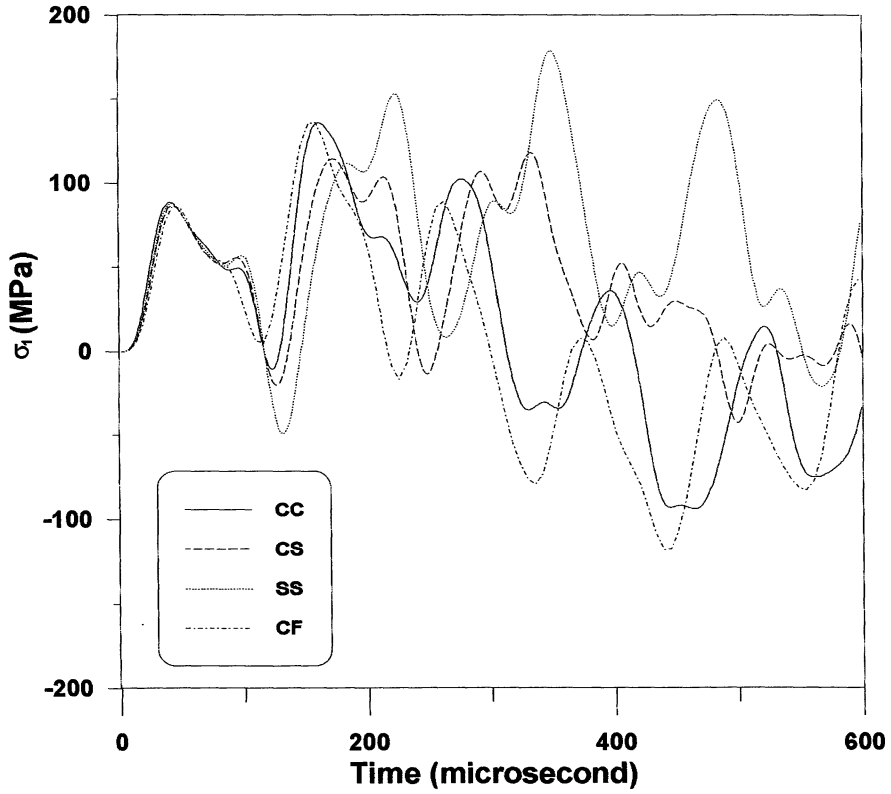

FIGURE 14 The histories of the inplane stresses in CC, CS, SS, and CF.

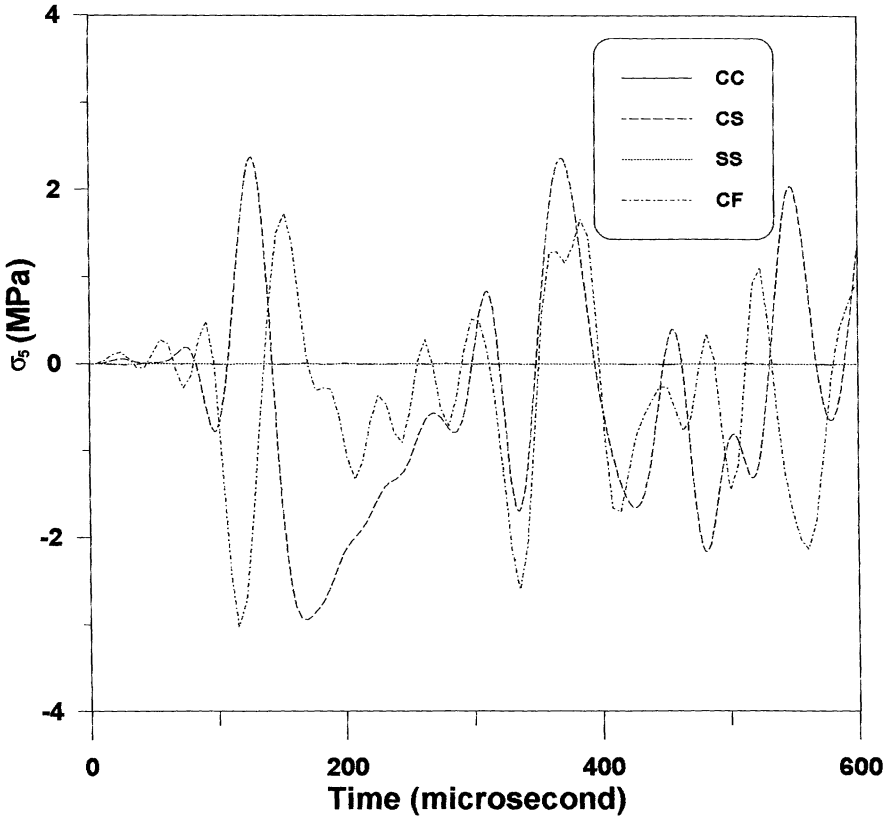

FIGURE 15 The histories of the transverse shear stresses in CC, CS, SS, and CF.

APPENDIX: MASS AND STIFFNESS MATRICES

The displacement u_0, w_0, and the rotation ψ_x can be expressed as

$$u_0 = \sum_{i=1}^{n} \phi_{ui}(x)A_i(t),$$
$$\psi_x = \sum_{i=1}^{n} \phi_{xi}(x)B_i(t), \qquad \text{(A.1)}$$
$$w_0 = \sum_{i=1}^{n} \phi_{zi}(x)C_i(t).$$

The stiffness matrix of the beam is given in the form

$$[K] = b\int_0^L \begin{bmatrix} K_{11} & K_{12} & K_{13} \\ K_{21} & K_{22} & K_{23} \\ K_{31} & K_{32} & K_{33} \end{bmatrix} dx, \qquad \text{(A.2)}$$

where

$$K_{mn} = K_{nm}^T, \quad K_{mn} = [k_{ij}^{mn}], \quad (m, n = 1, 2, 3),$$

and

$$k_{ij}^{11} = A_{11}\phi_{ui,1}\phi_{uj,1},$$
$$k_{ij}^{12} = \left(B_{11} - \frac{4E_{11}}{3h^2}\right)\phi_{ui,1}\phi_{xj,1},$$
$$k_{ij}^{13} = -\frac{4E_{11}}{3h^2}\phi_{ui,1}\phi_{zj,3},$$
$$k_{ij}^{22} = \left(A_{55} + \frac{16F_{55}}{h^4} - \frac{8D_{55}}{h^2}\right)\phi_{xi}\phi_{xj} + \left(D_{11} - \frac{8F_{11}}{3h^2} + \frac{16H_{11}}{9h^4}\right)\phi_{xi,1}\phi_{xj,1},$$
$$k_{ij}^{23} = \left(A_{55} + \frac{16F_{55}}{h^4} - \frac{8D_{55}}{h^2}\right)\phi_{xi}\phi_{zj,1} + \left(-\frac{4F_{11}}{3h^2} + \frac{16H_{11}}{9h^4}\right)\phi_{xi,1}\phi_{zj,3},$$
$$k_{ij}^{33} = \left(A_{55} + \frac{16F_{55}}{h^4} - \frac{8D_{55}}{h^2}\right)\phi_{zi,1}\phi_{zj,1} + \frac{16H_{11}}{9h^4}\phi_{zi,3}\phi_{zj,3}.$$

The mass matrix is in form of

$$[M] = b\int_0^L \begin{bmatrix} M_{11} & M_{12} & M_{13} \\ M_{21} & M_{22} & M_{23} \\ M_{31} & M_{32} & M_{33} \end{bmatrix} dx, \quad \text{(A.3)}$$

where

$$M_{kl} = M_{kl}^T, \quad M_{kl} = [m_{ij}^{kl}], \quad (k, l = 1, 2, 3),$$

and

$$\begin{aligned}
m_{ij}^{11} &= I_0\phi_{xi}\phi_{xj}, \\
m_{ij}^{12} &= \left(I_1 - \frac{4I_3}{3h^2}\right)\phi_{ui}\phi_{xj}, \\
m_{ij}^{13} &= -\frac{4I_3}{3h^2}\phi_{ui}\phi_{zj,1}, \\
m_{ij}^{22} &= \left(I_2 - \frac{8I_4}{3h^2} + \frac{16I_6}{9h^4}\right)\phi_{xi}\phi_{xj}, \\
m_{ij}^{23} &= \left(-\frac{4I_4}{3h^2} + \frac{16I_6}{9h^4}\right)\phi_{xi}\phi_{zj,1}, \\
m_{ij}^{33} &= I_0\phi_{zi}\phi_{zj} + \frac{16I_6}{9h^4}\phi_{zi,1}\phi_{zj,1}.
\end{aligned}$$

The coefficients in the matrixes $[K]$ and $[M]$ are defined as follows:

$$(A_{11}, B_{11}, D_{11}, E_{11}, F_{11}, H_{11}) = \sum_{k=1}^{K}\int_{h_{k-1}}^{h_k} Q_{11}^k(1, z, z^2, z^3, z^4, z^6)\, dz, \quad \text{(A.4a)}$$

$$(A_{55}, D_{55}, F_{55}) = \sum_{k=1}^{K}\int_{h_{k-1}}^{h_k} Q_{55}^k(1, z^2, z^4)\, dz, \quad \text{(A.4b)}$$

$$(I_0, I_1, I_2, I_3, I_4, I_6) = \sum_{i=1}^{K}\int_{h_{k-1}}^{h_k} \rho_k(1, z, z^2, z^3, z^4, z^6)\, dz. \quad \text{(A.4c)}$$

The third subscript in functions ϕ_{ui}, ϕ_{xi}, and ϕ_{zi} is defined as derivatives with respect to x:

$$(\ )_{,1} = \frac{\partial(\ )}{\partial x}, \quad (\ )_{,3} = \frac{\partial^2(\ )}{\partial x^2}. \quad \text{(A.5)}$$

REFERENCES

Bogdanovich, A. E., and Iarve, E. V., 1992, "Numerical Analysis of Impact Deformation and Failure in Composite Plates," *Journal of Composite Materials*, Vol. 26, pp. 520–545.

Cairns, D. S., and Lagace, P. A., 1989, "Transient Response of Graphite/Epoxy and Kevlar/Epoxy Laminates Subjected to Impact," *AIAA Journal*, Vol. 27, pp. 1590–1596.

Chattopadhyay, S., and Saxena, R., 1991, "Combined Effects of Shear Deformation and Permanent Indentation on the Impact Response of Elastic Plates," *International Journal of Solids and Structures*, Vol. 27, pp. 1739–1745.

Christoforou, A. P., and Swanson, S. R., 1991, "Analysis of Impact Response in Composite Plates," *International Journal of Solids and Structures*, Vol. 27, pp. 161–170.

Dobyn, A. L., 1981, "Analysis of Simply-Supported Orthotropic Plates Subject to Static and Dynamic Loads," *AIAA Journal*, Vol. 19, pp. 642–650.

Goldsmith, W., 1960, Impact: The Theory and Physical Behaviour of Colliding Solids, Edward Arnold, London.

Keer, L. M., and Balarini, R., 1983, "Smooth Contact Between a Rigid Indenter and an Initially Stressed Orthotropic Beam," *AIAA Journal*, Vol. 21, pp. 1035–1042.

Keer, L. M., and Lee, J. C., 1985, "Dynamic Impact of an Elastically Supported Beam—Large Area Contact. *International Journal of Engineering Science*, Vol. 23, pp. 987–997.

NAG, 1991, *NAG FORTRAN Library Manual*, Vol. 2. NAG, Wilkinson House, Oxford, U.K.

Rayleigh, J. W. S., 1906, "On the Production of Vibrations by Forces of Relatively Long Duration, with Applications to the Theory of Collisions," *The London, Edinburgh and Dublin Philosophical Magazine Series 6*, Vol. 11, p. 283.

Reddy, J. N., 1984, "A Simple Higher-Order Theory for Laminated Composite Plates," *AASME Journal of Applied Mechanics*, Vol. 51, pp. 745–752.

Schonberg, W. P., 1989, "Predicting the Low Velocity Impact Response of Finite Beams in Cases of Large Area Contact," *International Journal Impact Engineering*, Vol. 8, pp. 87–97.

Schonberg, W. P., Keer, L. M., and Woo, T. K., 1987, "Low Velocity Impact of Transversely Isotropic Beams and Plates," *International Journal of Solids and Structures*, Vol. 23, pp. 871–896.

Sun, C. T., *Analytical method for evaluation of impact damage energy of laminated composites*, ASTM STP Series 617, 1977, ASTM Philadelphia, PA, pp. 427–440.

Sun, C. T., and Chattopadhyay, S., 1975, "Dynamic response of anisotropic laminated plates under initial stress to impact of a mass," *ASME Journal of Applied Mechanics*, Vol. 42, pp. 693–698.

Timoshenko, S. P., 1931, "Zur frage Nach der Wirkung Eines Stosse auf Einer Balken," *Zeitschrift für Mathematische und Physik*, Vol. 62, pp. 198–209.

Timoshenko, S. P., and Young, D. H., (1954), *Vibration problems in engineering, 3rd* ed., Van Nostrand Reinhold, New York, pp. 411–416.

Xia, Y., (1988), Behaviour of a two-layered beam under impact loading, *International Journal Impact Engineering*, Vol. 7, pp. 415–428.

Yang, S. H., and Sun, C. T., Indentation law for composite laminates, in I. M. Daniel, *Composite Materials: Testing and Design*, ASTM STP 787, 1982, pp. 425–449.